INTERNATIONAL JOURNAL OF INTEGRATED ENGINEERING
ISSN: 2229-838X e-ISSN: 2600-7916

IJIE

Vol. 16 No. 2 (2024) 195-202
https://publisher.uthm.edu.my/ojs/index.php/ijie

Corrosion Behaviour of Stainless Steel 316L in Chloride Environment After Dry Machining by Face Milling at Various Spindle Speed

Teguh Dwi Widodo[1]*, Rudianto Raharjo[1], Redi Bintarto[1], Lucky Haris Suharto[1], Arif Wahyudiono[2], Fikrul Akbar Alamsyah[1,3]

[1] *Mechanical Engineering Department, Brawijaya University, Jl. MT Haryono No. 167, Malang, 65145, INDONESIA*
[2] *Mechanical Engineering Department, Malang State University, Jl. Cakrawala No.5, Malang,65145, INDONESIA*
[3] *Mechanical and Electro-Mechanical Engineering Department, National Sun Yat-sen University, Lianhai Rd No. 70, Kaohsiung City 82445, TAIWAN*

*Corresponding Author: widodoteguhdwi@ub.ac.id
DOI: https://doi.org/10.30880/ijie.2024.16.02.020

Article Info

Received: 14 December 2023
Accepted: 4 April 2024
Available online: 30 May 2024

Keywords

Dry machining, corrosion, surface roughness, spindle speed, stainless steel 316L

Abstract

This study attempts to investigate the impact of spindle speed on the corrosion characteristics of 316L stainless steel during the face milling process in dry condition. The machining parameters, such as spindle speed, have an impact on the surface properties of the material after the processes. It is essential to devote significant attention that these parameters can still affect the surface condition of 316L stainless steel, which may then affect its corrosion properties. This research aimed to examine the corrosion characteristics of 316L stainless steel subsequent to the face milling process using the potentiodynamic polarization technique in a chloride-containing environment. The face milling technique use a 6 mm carbide cutter tool, with spindle speed variations of 1800 rpm, 1600 rpm, and 1400 rpm. The feed rate is maintained in constant rate, which is 0.002 mm/rev. The findings of the corrosion rate test indicate that variations in spindle speed lead to fluctuations in the corrosion rate value. There finding shows an inverse relationship between the value of spindle speed and the corrosion rate, wherein an increase in spindle speed corresponds to a decrease in the corrosion rate.

1. Introduction

Stainless steels are alloys primarily composed of iron and chromium, with a minimum chromium content of roughly 12%. The corrosion resistance of the steel is attributed to the presence of a thin, adherent, passive layer that forms on its surface. This film acts as a barrier, slowing or preventing the progression of corrosion. A lot of research has already shown that passive films made on stainless steel have a lot more chromium than they should. This chromium is usually found as hydrated oxide or hydroxide compounds. When stainless steels are subjected to environments that include halide ions, such as saltwater, the passive behavior of certain areas might transition from a passive state. As a result, localized corrosion phenomena, such as crevice corrosion and/or pitting, may manifest.

Pitting corrosion is a common phenomenon that arises when metals are subjected to a corrosive environment containing highly reactive ions, with chloride being the predominant factor in the majority of instances [1]–[6]. In a broad sense, the pitting corrosion mechanism of metals immersed in solutions containing

chloride ions may be described as a series of four sequential stages: initial production of a protective passive layer, subsequent breakdown of the passive film, development of metastable pits that have the ability to undergo re-passivation, and eventual growth of stable pits [7]–[8]. Nevertheless, it exhibits a significant susceptibility to pitting corrosion when exposed to acidic conditions containing chloride ions. The presence of an acidic environment leads to the degradation of the film layer and the production of significant pitting [9]-[11]. The drop in pH value of a solution results in a reduction in the charge transfer resistance of the oxide layer. This reduction leads to an increase in the ratio of OH^-/O_2^- and an increase in its disorder. Consequently, the occurrence of pitting corrosion becomes more severe.

Numerous researchers have extensively conducted a range of procedures, including cathode protection, inhibitor protection, coating, and alloying element addition, in order to safeguard metals from pitting corrosion [12]–[13]. Nevertheless, the implementation of these procedures is consistently hindered by the myriad complexities inherent in their actual application. The process of material selection and manufacturing plays a crucial role in determining the suitable alloys that possess the necessary corrosion resistance for a certain application in various environmental conditions, particularly when corrosion resistance is the primary criterion. The surface qualities of the material are highly influenced by the manufacturing or machining process, then this surface quality leads to corrosion properties. However, the utilization of mineral oil which is widely used in the manufacturing process attracts special attention due to environmental concerns [14]-[15].

Dry machining method is attracting special attention due to environmental issue. In this machining method, the process did not employ cutting fluid where recently this fluid has become an environmental problem because generally this cutting fluid derived from mineral base oil. However, dry machining also results in negative effects in surface properties, like surface roughness, deformation, and corrosion. Surface roughness measurement is a crucial aspect of the production process that ensures the quality of face-milled components. Surface roughness assessment plays a crucial role in the evaluation of machinability since it is considered a significant performance feature. In contemporary times, industrial companies place significant emphasis on achieving a high-quality surface finish during machining operations [16]–[20].

Stainless steel is widely utilized in engineering systems due to its versatility and cost-effectiveness. One of the primary drawbacks associated with stainless steel is its ability to resist corrosion, particularly in moderate operating conditions. Various approaches can be employed to address the issue of corrosion and prolong the lifespan of the components. The identification and implementation of optimal process parameters for machining operations is a significant factor to be considered. To optimize the efficiency of machined samples, it is imperative to enhance their functional qualities through the careful selection of suitable face milling settings. The purpose of this study is to reveal the effect of spindle speed on the face milling process of stainless steel 316L with dry method on corrosion behavior in a chloride environment.

2. Methodology

Stainless steel 316L is used as specimen in this study which the chemical composition is shown in Table 1. The cutting tool material used is carbide end mills as tools supplied by Nachi VG Mill Japan. The face milling process was utilized HAAS VF2. Before face milling was applied to the material, the material was subjected to cutting using a shearing machine with dimensions of 4 cm by 10 cm. The experiment diagram of milling process is shown in figure 1.

Table 1 *Chemical composition of stainless steel 316L*

C	Mn	P	S	Si	Mo	N	Fe	Cr	Ni
0.03	2	0.045	0.03	0.75	2.2	0.1	67.8	16.7	12.4

The face milling process varied in spindle speed 1800 rpm, 1600 rpm, and 1400 rpm with constant feed rate 0,002 mm/rev. The face milling processes was using dry method. This method provides less environmental impact as residual effect in machining processes. The surface roughness of the face milled components is evaluated by Mitutoyo surf test SJ 301 roughness testing machine. The surface roughness is measured three times for the samples and average value is considered for investigation.

The corrosion rate and current density are measured by potential dynamic polarization technique at room temperature and 0.5 mV/s scan rate, using electrochemical cell which contains three cells. These three-electrode cells consist of stainless steel 316L as working electrode, saturated Ag/AgCl as reference electrode, and platinum as counter electrode. The machined samples are cleaned with distilled water and acetone prior to being exposed in corrosion test. Specimens are attached to a holder and kept exposed to the testing environment to achieve maximum exposure of 1 cm2 surface area, followed by dipping in 5 %wt NaCl solution. The corrosion test was taking place in room temperature and the experiment set up is shown in figure 2.

Int. Journal of Integrated Engineering Vol. 16 No. 2 (2024) p. 195-202

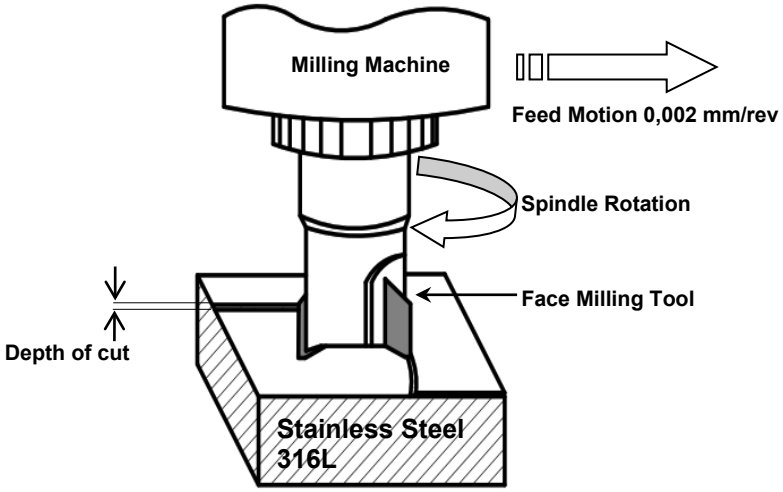

Fig. 1 *Experimental diagram of face milling*

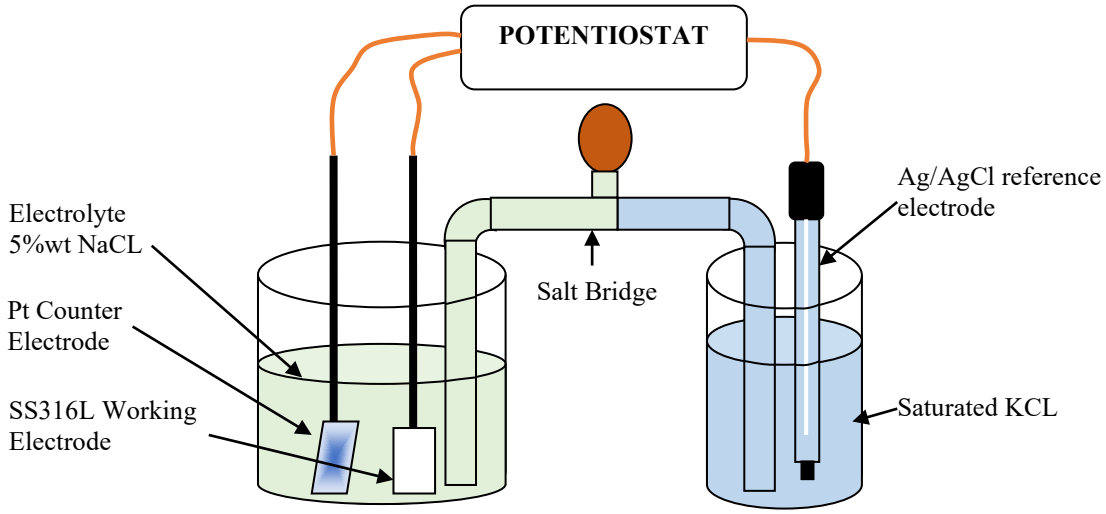

Fig. 2 *Experimental setup of potentitiodynamic polarization*

3. Results

3.1 Surface Roughness

Table 2 shows the surface roughness data of stainless steel 316 L after process face milling with various spindle speeds. Three samples were taken for each variation and then averaged to obtain comprehensive data. Meanwhile, the correlation between mean surface roughness of the face milled stainless steel 316L with various spindle speed is shown in figure 3. The data reveals that the higher spindle speed provides lower surface roughness, as indicated by a Ra value 1.757 µm for 1400 rpm, 1.534 µm for 1600 rpm, and 1.352 µm for 1800 rpm.

The data show that at spindle speed 1800 rpm the surface roughness tends to lowest value, it has mean that at that spindle speed cutting tools still able to cut stainless steel 316 L may without any damage or severe deformation on the surface. Theoretically, increasing spindle speed will increase the milling process's energy consumption. This energy will be transferred to the specimen by the cutting instrument in the form of heat or force, which, if exceeded, may cause deformation.

Table 2 *Surface roughness of stainless steel 316 L after face milling*

No.	*Spindle Speed* (rev/minutes)	Ra (µm)	Mean Ra (µm)
1	1800	1.330	1.352
2		1.361	
3		1.365	
1	1600	1.536	1.534
2		1.546	
3		1.519	
1	1400	1.763	1.757
2		1.742	
3		1.767	

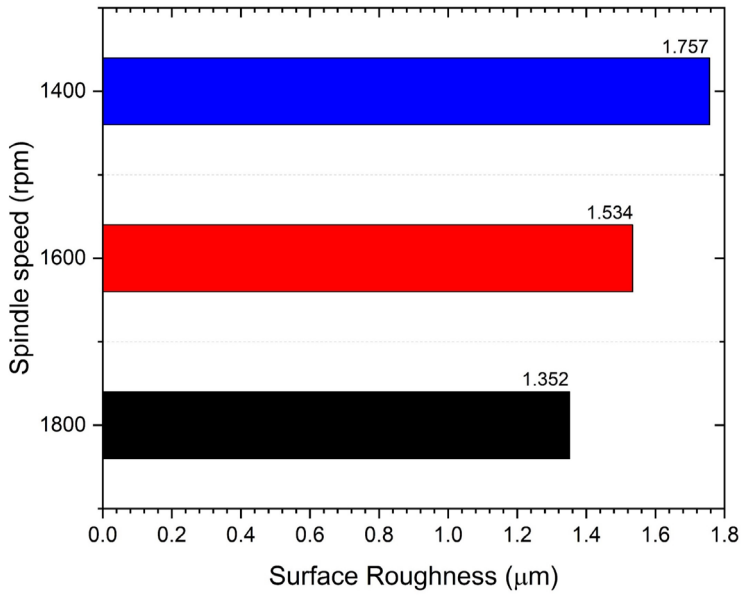

Fig. 3 *Surface roughness of face milled stainless steel 316L with different spindle speed (a) 1400 rpm; (b) 1600 rpm; (c) 1800 rpm*

3.2 Corrosion Properties

Table 3 shows the Tafel plot form potentiodynamic polarization test results of stainless steel 316L in 5% NaCl following face milling with varying spindle speeds which is derivate from potentiodynamic polarization curve. Meanwhile, potentiodynamic polarization curves of stainless steel 316L after face milled in dry condition is shown in figure 4.

Table 3 *Parameters of polarization curves for various specimen in 5% wt NaCl*

Spindle Speed (rpm)	$\beta_{cathode}$ (mV/decade)	β_{anode} (mV/decade)	Polarization Resistance (Ω)	E_{corr} (V)	i_{corr} (µA/cm^2)	Corrosion Rate (mm/year)
1400	143.380	86.170	2.59 x 10^3	-1.201	18.021 x 10^{-6}	0.403
1600	103.240	71.889	3.51 x 10^3	-1.015	10.598 x 10^{-6}	0.237
1800	115.040	96.745	4.31 x10^3	-0.932	10.481 x 10^{-6}	0.234

The test was recorded in a solution of 25 °C and 5% wt NaCl at scan rates 1mV/s. Anodic polarization of the sample behaved like any other stainless steel 316L in a NaCl solution, with cathodic reaction (stage 1), active dissolution (stage 2), passivity (stage 3), and a rapid dissolution (stage 4). The polarization demonstrates that the corrosion potential shifted from less noble (less Ecorr) to more noble (high Ecorr) in materials face-milled at

Int. Journal of Integrated Engineering Vol. 16 No. 2 (2024) p. 195-202

greater spindle speeds. The Nobler substance refers to the less active substance. Moreover, as the spindle speed increases, the current density decreases. There is a direct correlation between the current density and the corrosion rate, with a higher current density resulting in a higher corrosion rate. Meanwhile, in the right part of the polarization data there is rapid dissolution which is identified by the fast rise in the current density, which shows that steady pitting is happening. The potential that matches this current transition is called a critical pitting potential, or Epit [1]. The Epit data show by increasing the spindle speed, the Epit shift to more noble, which can be interpreted the surface has better pitting corrosion resistance.

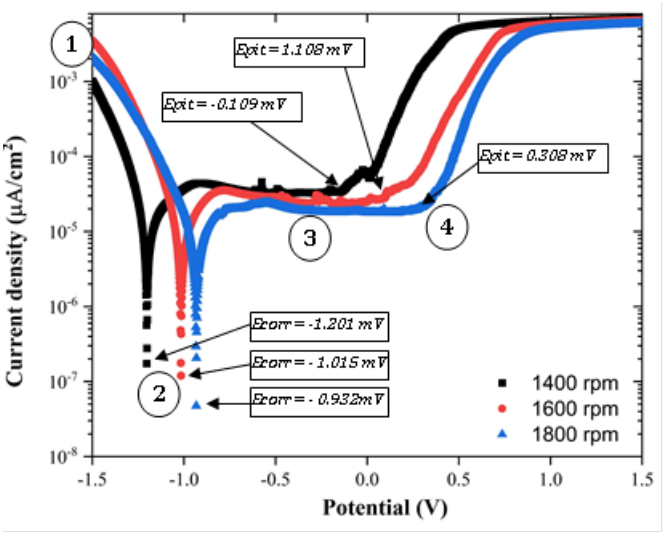

Fig. 4 *Polarization curves of face milled stainless steel 316L with different spindle speed (a) 1400 rpm; (b) 1600 rpm; (c) 1800 rpm*

3.3 Surface Characterization

The scanning electron microscope (SEM) of the samples prior to and after the corrosion process is shown in figure 5.

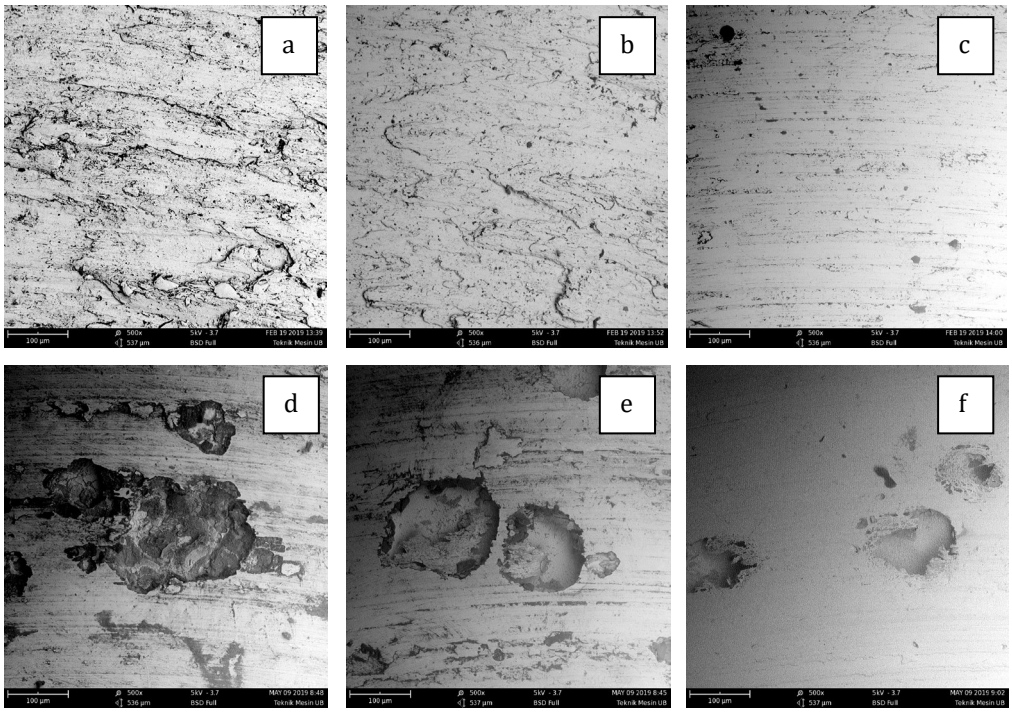

Fig. 5 *SEM image of face milled stainless steel 316L with different spindle speed prior (a) 1400 rpm; (b) 1600 rpm; (c) 1800 rpm and after corrosion test; (d) 1400 rpm; (e) 1600 rpm; (f) 1800 rpm*

The SEM image shows that the surface topography varied with the different spindle speeds. The image shows different topography in three different samples. The higher spindle speed in the face milling process leads to less deformation on the surface of the stainless steel 316L as shown in figure 5c compared to less spindle speed as shown in figure 5a and 5b. The surface deformation is clearly seen in the specimen, which was face milled at 1400 rpm.

Figures 5d, 5e, 5f show the observation result after the corrosion test. The observation presence of stable pits that have developed throughout the polarization process. These phenomena are supported by potentiodynamic polarization found in figure 4 which displays the presence of current density spikes occurring at transpassive point. The presence of spikes in the data can be attributed to the existence of metastable pits, which can be further elucidated by the successive production and re-passivation of micro size pits. The Pit form shows the difference in size between low spindle speed and high spindle speed. At low spindle speed it can observed that the pit form tends wider than high spindle speed.

4. Discussion

From figure 3, the results of effect spindle speed on surface roughness, which the higher the spindle speed used, the smaller the surface roughness value is obtained. This is because the large spindle rotation causes the cut intensity to increase in same feed distance, as a result the workpiece is cut repeatedly so that the surface of the workpiece becomes smoother. And conversely, small rotations cause less cut intensity, as a result the workpiece is cut less repeatedly so that the surface roughness becomes greater. The impact of spindle rotation speed on cut surface overlap can be shown in figure 6 and illustrated in figure 7. The workpiece surface exhibits a significant number of incision intensities in the 1800 rpm variation, which may be contrasted with the spindle speeds of 1600 rpm and 1400 rpm. It is evident that a drop in spindle speed results in a reduction in cutting intensity, as indicated by fewer scratches relative to the fluctuations at 1600 rpm and 1800 rpm. This result is detailed supported by the SEM result, which is shown in figure 5a, 5b, 5c. The higher the spindle speed value, the fewer streaks, cracks, and scratches resulting from machining will appear on the surface. This SEM data strengthening reason that at the higher the spindle speed, the higher the incision intensity is take place resulting smoother surface.

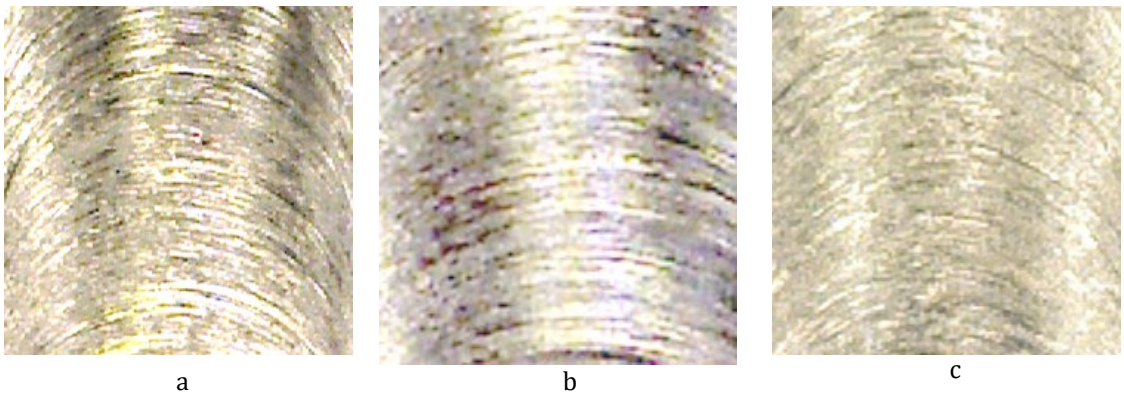

Fig. 6 *Illustration of cut surface overlap in various spindle speed (a) 1400 rpm; (b) 1600 rpm; (c) 1800 rpm*

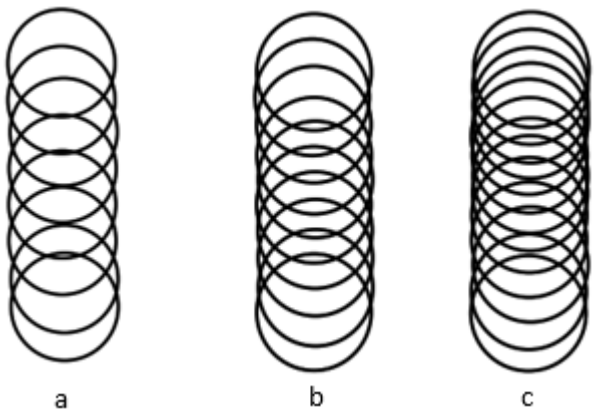

Fig. 7 *Illustration of cut surface overlap in various spindle speed (a) 1400 rpm; (b) 1600 rpm; (c) 1800 rpm*

Int. Journal of Integrated Engineering Vol. 16 No. 2 (2024) p. 195-202

Visualization of the specimen prior to and after corrosion test was shown in figure 5. The most obvious difference is that after corrosion testing, corrosion appears in the form of pitting corrosion on the test object's surface. As previously discussed, the increasing surface roughness of the surface of the test object is due to decreasing spindle speed. Increasing surface roughness led to decrease the corrosion potential (Ecorr) and increase the corrosion rate. The corrosion current increases as the decrease spindle speed, it may because the decrement in spindle speed led to increase the surface roughness (figure 3) in which with higher surface roughness increase the real corroded surface area. Meanwhile the recorded corrosion area is the same for every sample. The correlation between surface and the corrosion rate is shown in equation 1.

$$r = \frac{i_{corr}\, x\, M}{nF\rho} \tag{1}$$

Where i_{corr} is current density (μA/cm^2), M is atomic mass (g/mol), n is electron valence number, F is Faraday's constant number 96485 C/mol, ρ is density of corroded material (g/cm^3). From the equation, surface area affects the current density. For example, when the area of the corroded material is recorded as 450 μm by 450 μm, the actual area is more than 450 μm by 450 μm because there are valleys and hills, which increase the surface area as shown in the 3D image of the face milled surface in figure 7. On the other hand, the machine only records the current value and does not record the current density. To obtain current density data, the recorded current is divided by surface area, which makes the recorded surface area smaller that actual area, resulting in higher current density.

The number of valleys and hills decrease as increase the spindle speed increase which effects the decrease the corrosion current density. The decrement of the corrosion current density naturally decreases the corrosion rate. Meanwhile the corrosion potential (E_{corr}) shift to less noble as decrease the spindle speed. It may be attributed to the irregularity of the surface sample, which leads to the instability of passive film on the surface of stainless steel 316L. The correlation of the surface irregularly and electrochemical activity was reported by Li et all [20]. This correlation is shown with equation 2.

$$\Delta\varphi^{\circ} = -\frac{\Delta P V_m}{nF} \tag{2}$$

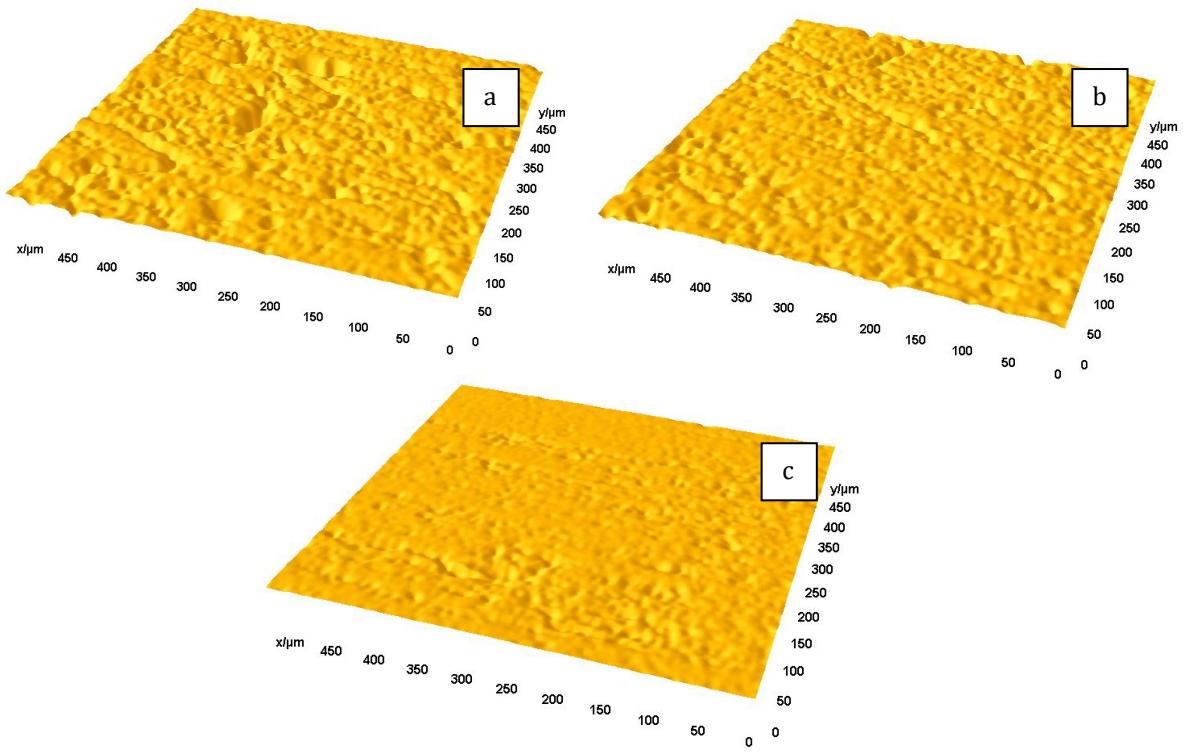

Fig. 8 *3D image of face milled stainless steel 316L with different spindle speed prior and after corrosion test (a) 1400 rpm; (b) 1600 rpm; (c) 1800 rpm*

Where $\Delta\varphi^{\circ}$ is change of electrode potential and ΔP is excessive pressure resulted from local stress concentration and is the molar volume of the sample. Decrease in surface irregularity produced during face milling processes will lead to increased stress concentration, thereby resulting in a bigger value of in equation 1. As the degree of stress concentration increases, the change of electrode increases. As a result, the potential of the steel becomes more negative. At lower spindle speed the stress concentration may increase due to the machining process needs more force to cut the specimen at same feed rate compared to high spindle speed. In this study, pitting corrosion was also identified in the surface samples. Although stainless steel 316L is difficult to corrode due to its chromium, nickel, and molybdenum content, which forms a protective layer, the electrode potential is shifting to negative caused by surface frugality and chloride ion attack [21]. The pitting corrosion takes place on the stainless steel 316L surface. The chloride ion helps the electrolyte damage the passive layer. This damage initiates a pitting corrosion attack on the sample surface. This is also supported by the statement that high surface roughness is often attacked by pitting corrosion [21]-[5].

5. Conclusion

The rotational speed of the spindle during the machining process plays an important role in dry machining. The higher spindle speed led to a reduction in surface roughness, resulting in smoother surfaces and a lower incidence of scratches and cracks. On the other hand, the reduction in spindle speed tends to elevate surface roughness, resulting in the occurrence of pitting corrosion and a subsequent decline in corrosion potential. The lower spindle speed may increase the stress concentration on the substrate, which may lead to the potential of the substrate shifting to a less noble state. The pitting corrosion on the face milled sample may be caused by the combination effect of surface roughness and the presence of chloride ions.

Acknowledgement

The authors would like to express thankfulness to Brawijaya University for their research funding and facility support.

Conflict of Interest

Authors declare that there is no conflict of interests regarding the publication of the paper.

Author Contribution

Study conception and design: *Teguh Dwi Widodo;* ***data collection:*** *Lucky Haris Suharto, Arif Wahyudiono, Fikrul Akbar Alamsyah,;* ***analysis and interpretation of results:*** *Teguh Dwi Widodo, Rudianto Raharjo, Redi Bintarto,;* ***draft manuscript preparation:*** *Teguh Dwi Widodo, Rudianto Raharjo, Arif Wahyudiono.*

References

[1] Ak Xin, S. S., & Li, M. C. (2014). Electrochemical corrosion characteristics of type 316L stainless steel in hot concentrated seawater. Corrosion Science, 81, 96–101. https://doi.org/10.1016/J.CORSCI.2013.12.004

[2] Li, L., Qiao, Y., Zhang, L., Ma, A., Daniel, E. F., Ma, R., Chen, J., & Zheng, Y. (2023). Effect of surface damage induced by cavitation erosion on pitting and passive behaviors of 304L stainless steel. *International Journal of Minerals, Metallurgy and Materials*, *30*(7), 1338–1352. https://doi.org/10.1007/s12613-023-2602-0

[3] Yang, Y., Li, M., & Zhou, Q. (2023). Corrosion performance of typical stainless steels in concentrated seawater under vacuum and boiling condition. *International Journal of Electrochemical Science*, *18*, 100387. https://doi.org/10.1016/j.ijoes.2023.100387

[4] Bai, H., Cui, X., Wang, R., Lv, N., Yang, X., Li, R., & Ma, Y. (2023). Effect of Surface Roughness on Static Corrosion Behavior of J55 Carbon Steel in CO2-Containing Geothermal Water at 65 °C. *Coatings*, *13*(5). https://doi.org/10.3390/coatings13050821

[5] He, W., Knudsen, O., & Diplas, S. (2009). Corrosion of stainless steel 316L in simulated formation water environment with CO2–H2S–Cl–. *Corrosion Science*, *51*(12), 2811–2819. https://doi.org/10.1016/J.CORSCI.2009.08.010

[6] Widodo, T. D., Raharjo, R., Bintarto, R., Wahyudiono, A., & Alamsyah, F. A. (2023). Effect of Stand of Distance (SOD) of Abrasive Water Jet Cutting Processes on the Corrosion Properties of Material Implant Stainless Steel 316L. In *Key Engineering Materials* (Vol. 940, pp. 107–113). Trans Tech Publications Ltd. https://doi.org/10.4028/p-jz3zcd

[7] Li, T., Scully, J. R., & Frankel, G. S. (2019). Localized Corrosion: Passive Film Breakdown vs. Pit Growth Stability: Part IV. The Role of Salt Film in Pit Growth: A Mathematical Framework. *Journal of The Electrochemical Society*, *166*(6), C115–C124. https://doi.org/10.1149/2.0211906jes

[8] Scheiner, S., & Hellmich, C. (2007). Stable pitting corrosion of stainless steel as diffusion-controlled dissolution process with a sharp moving electrode boundary. *Corrosion Science*, *49*(2), 319–346. https://doi.org/10.1016/J.CORSCI.2006.03.019
[9] Ge, H. H., Xu, X. M., Zhao, L., Song, F., Shen, J., & Zhou, G. D. (2011). Semiconducting behavior of passive film formed on stainless steel in borate buffer solution containing sulfide. *Journal of Applied Electrochemistry*, *41*(5), 519–525. https://doi.org/10.1007/S10800-011-0272-5/FIGURES/8
[10] Bai, P., Zheng, S., Zhao, H., Ding, Y., Wu, J., & Chen, C. (2014). Investigations of the diverse corrosion products on steel in a hydrogen sulfide environment. *Corrosion Science*, *87*, 397–406. https://doi.org/10.1016/J.CORSCI.2014.06.048
[11] Wang, Z., Zhang, L., Tang, X., Zhang, Z., & Lu, M. (2017). The surface characterization and passive behavior of Type 316L stainless steel in H2S-containing conditions. *Applied Surface Science*, *423*, 457–464. https://doi.org/10.1016/J.APSUSC.2017.06.214
[12] Hayatdavoudi, H., & Rahsepar, M. (2017). A mechanistic study of the enhanced cathodic protection performance of graphene-reinforced zinc rich nanocomposite coating for corrosion protection of carbon steel substrate. *Journal of Alloys and Compounds*, *727*, 1148–1156. https://doi.org/10.1016/j.jallcom.2017.08.250
[13] Pourhashem, S., Saba, F., Duan, J., Rashidi, A., Guan, F., Nezhad, E. G., & Hou, B. (2020). Polymer/Inorganic nanocomposite coatings with superior corrosion protection performance: A review. In *Journal of Industrial and Engineering Chemistry* (Vol. 88, pp. 29–57). Korean Society of Industrial Engineering Chemistry. https://doi.org/10.1016/j.jiec.2020.04.029
[14] Schwarz, M., Dado, M., Hnilica, R., & Veverková, D. (2015). Environmental and Health Aspects of Metalworking Fluid Use. In *J. Environ. Stud* , 24(1), 37-45. https://doi.org/10.1002/jsl.3000140104
[15] Lennartz, J., Toxopeus, M. E., & Meulen, J. Van Der. (2022). Analysis of environmental transitions for tool development. *Procedia CIRP*, *105*, 799–804. https://doi.org/10.1016/j.procir.2022.02.132
[16] Li, W., & Li, D. Y. (2005). Variations of work function and corrosion behaviors of deformed copper surfaces. *Applied Surface Science*, *240*(1–4), 388–395. https://doi.org/10.1016/j.apsusc.2004.07.017
[17] Sharma, A., Chawla, H., & Srinivas, K. (2023). Prediction of Surface Roughness of Mild Steel finished with Viscoelastic Magnetic Abrasive Medium. In *EVERGREEN Joint Journal of Novel Carbon Resource Sciences & Green Asia Strategy* 10(2), 942-952. https://doi.org/10.5109/6792889
[18] Hussain, M., & Schaus, D. (2022). Effect of surface roughness and coating alternatives of seawater pipes on energy efficiency of ships. *International Journal of Energy and Water Resources*, *6*(2), 183–193. https://doi.org/10.1007/s42108-021-00164-y
[19] Gupta, P., Singh, B., & Shrivastava, Y. (2023). Theoretical and Experimental Prediction of Optimal Process Variables for Enhanced Metal Removal Rate During Turning on CNC lathe. In *EVERGREEN Joint Journal of Novel Carbon Resource Sciences & Green Asia Strategy* ,10(2), 1127-1132. https://doi.org/10.5109/6793673
[20] Li, Y., & Cheng, Y. F. (2016). Effect of surface finishing on early-stage corrosion of a carbon steel studied by electrochemical and atomic force microscope characterizations. *Applied Surface Science*, *366*, 95–103. https://doi.org/10.1016/j.apsusc.2016.01.081
[21] McCafferty, E. (2003). Sequence of steps in the pitting of aluminum by chloride ions. *Corrosion Science*, *45*(7), 1421–1438. https://doi.org/10.1016/S0010-938X(02)00231-7
[22] Croll, S. G. (2020). Surface roughness profile and its effect on coating adhesion and corrosion protection: A review. In *Progress in Organic Coatings* (Vol. 148). Elsevier B.V. https://doi.org/10.1016/j.porgcoat.2020.105847
[23] Bai, H., Cui, X., Wang, R., Lv, N., Yang, X., Li, R., & Ma, Y. (2023). Effect of Surface Roughness on Static Corrosion Behavior of J55 Carbon Steel in CO2-Containing Geothermal Water at 65 °C. *Coatings*, *13*(5). https://doi.org/10.3390/coatings13050821
[24] Reddy, U., Dubey, D., Panda, S. S., Ireddy, N., Jain, J., Mondal, K., & Singh, S. S. (2021). Effect of Surface Roughness Induced by Milling Operation on the Corrosion Behavior of Magnesium Alloys. *Journal of Materials Engineering and Performance*, *30*(10), 7354–7364. https://doi.org/10.1007/s11665-021-05933-8
[25] Luo, K., Xing, Y., Sun, M., Xu, L., Xu, S., Wang, C., & Lu, J. (2023). Effect of laser shock peening on the dissolution of precipitates and pitting corrosion of AA6061-T6 with different original surface roughness. *Corrosion Science*, 111794. https://doi.org/10.1016/j.corsci.2023.111794